

Monolithic ATF MiniFuel Sample Capsules Ready for HFIR Insertion

**Nuclear Technology
Research and Development**

Approved for public release.
Distribution is unlimited.

***Prepared for
US Department of Energy
Advanced Fuels Campaign
C.M. Petrie, A.G. Le Coq,
M.D. Richardson, C.A. Hobbs,
G.W. Helmreich, J.R. Burns, J.M. Harp
Oak Ridge National Laboratory***

January 17, 2020

NTRD: M2FT-20OR020203042



DISCLAIMER

This information was prepared as an account of work sponsored by an agency of the U.S. Government. Neither the U.S. Government nor any agency thereof, nor any of their employees, makes any warranty, expressed or implied, or assumes any legal liability or responsibility for the accuracy, completeness, or usefulness, of any information, apparatus, product, or process disclosed, or represents that its use would not infringe privately owned rights. References herein to any specific commercial product, process, or service by trade name, trade mark, manufacturer, or otherwise, does not necessarily constitute or imply its endorsement, recommendation, or favoring by the U.S. Government or any agency thereof. The views and opinions of authors expressed herein do not necessarily state or reflect those of the U.S. Government or any agency thereof.

SUMMARY

Several advanced nuclear fuel concepts are being considered throughout the nuclear industry. Implementation of these concepts could increase accident tolerance or enhance performance beyond the capabilities of the UO_2 -based nuclear fuel currently in use. Qualification and deployment of any new fuel requires rigorous irradiation testing to demonstrate performance under representative normal and off-normal operating conditions. The traditional approach for qualifying new fuels requires exhaustive execution of many integral fuel tests. However, due to the long timeframe for executing these integral tests and the limited number of available materials test reactors, this approach is becoming impractical. To accelerate fuel qualification, Oak Ridge National Laboratory developed the MiniFuel irradiation vehicle for use in conducting accelerated separate effects irradiation testing of a wide range of nuclear fuel materials in the High Flux Isotope Reactor (HFIR). The first MiniFuel irradiations performed in the facility tested sol gel-derived uranium nitride kernels and tristructural isotropic (TRISO)-coated particle fuels. This report describes the preparation and assembly of the first set of monolithic MiniFuel irradiations conducted to support accident-tolerant fuel (ATF) development and accelerated fuel qualification. Two irradiation targets containing a variety of UO_2 and U_3Si_2 disk fuel specimens were fabricated and assembled for irradiation to burnups of 8–10 and 28–40 MWd/kg U. The target irradiation temperature is 450–550°C. Irradiation of U_3Si_2 will provide new data regarding the irradiation performance of a candidate ATF to complement current ATF-1 integral experiments being performed in the Advanced Test Reactor. UO_2 samples were included as a reference so that the results from the MiniFuel experiments can be compared with the extensive UO_2 fuel performance database. The monolithic MiniFuel capsules were successfully assembled, welded, and tested per HFIR requirements and are ready for insertion into the reactor. Pictures of the assembly process are included in this report. The experiment is planned for insertion into the HFIR during cycle 487 in April 2020.

CONTENTS

SUMMARY	iii
ACRONYMS AND ABBREVIATIONS	ix
ACKNOWLEDGMENTS	x
1. INTRODUCTION	1
2. EXPERIMENT DETAILS	2
2.1 Fuel configuration and test matrix	2
2.2 Pre-irradiation characterization	4
3. EXPERIMENT ANALYSIS RESULTS	7
3.1 Burnup calculations	7
3.2 Thermal analyses	8
4. EXPERIMENT FABRICATION	11
5. PLANNED POST-IRRADIATION EXAMINATION	14
6. SUMMARY AND CONCLUSIONS	15
7. REFERENCES	15
APPENDIX A. FABRICATION DOCUMENTATION FOR EXPERIMENTS	A-1

FIGURES

Figure 1. MiniFuel experiment configuration showing sealed capsules with disk specimens (this work), as well as other potential fuel configurations. This figure was reused with permission from Petrie et al. [2].	2
Figure 2. Pictures of the U_3Si_2 disk specimens [6].	3
Figure 3. Pictures of the UO_2 disk specimens.	3
Figure 4. Percent theoretical densities for the UO_2 specimens determined using geometric measurements (ORNL Geo), XCT, and a 3D Keyence optical profilometer (Keyence). Only the last two digits of the specimen IDs are shown.	6
Figure 5. Percent theoretical densities for the U_3Si_2 specimens determined using geometric measurements (ORNL Geo and LANL Geo), immersion (LANL Immersion), XCT, and a 3D Keyence optical profilometer (Keyence). Only the last two digits of the specimen IDs are shown. Keyence measurements for specimens 52 and 54 are off scale and clearly nonphysical ($>100\%$ theoretical density).	6
Figure 6. Calculated U_3Si_2 fuel fission rate (solid lines) and burnup (dashed lines) vs. irradiation time or number of HFIR cycles for the first 4 cycles of irradiation in capsules with RAS IDs 121, 123, 124, and 126. R = radial target position, A = axial target position, and S = subcapsule (or capsule) position.	8
Figure 7. Predicted temperature contours (in $^{\circ}C$) for a U_3Si_2 disk specimen in position RAS 123 at the end of 4 cycles of irradiation. Results show the capsule assembly (top) and the fuel specimen (bottom).	9
Figure 8. Calculated variations in the average U_3Si_2 disk fuel temperatures (top) and TM temperatures (bottom) at beginning of cycle (BOC) and end of cycle (EOC) for cycles 1, 4, and 12.	10
Figure 9. Components for one UO_2 -fueled capsule.	11
Figure 10. Loading of a UO_2 disk specimen (a) into a cup inside the bottom loading fixture (b).	12
Figure 11. Filler placed over cup assembly and turned upside down while applying pressure with top loading fixture (a), bottom loading fixture removed (b), and capsule is turned upside down and placed over the tube and cup assembly (c).	12
Figure 12. Loading TMs (a), insulators (b), and endcaps (c) into a capsule.	13
Figure 13. All 12 capsules prepped for electron beam welding (a); close-up views of a single capsule before (b) and after (c) welding.	13

TABLES

Table 1. Test matrix for U_3Si_2 and UO_2 monolithic disk irradiation.....	4
Table 2. Pre-irradiation mass and dimensional measurements of specimens.	5

ACRONYMS AND ABBREVIATIONS

AFC	Advanced Fuels Campaign
ATF	accident tolerant fuel
BOC	beginning of cycle
DOE-NE	US Department of Energy, Office of Nuclear Energy
EOC	end of cycle
HFIR	High Flux Isotope Reactor
IFEL	Irradiated Fuels Examination Laboratory
LANL	Los Alamos National Laboratory
ORNL	Oak Ridge National Laboratory
PIE	post-irradiation examination
SiC	silicon carbide
TM	temperature monitor
TRISO	tristructural isotropic
UN	uranium nitride
UO ₂	uranium dioxide
U ₃ Si ₂	uranium silicide
XCT	x-ray computed tomography

ACKNOWLEDGMENTS

This work was supported by the US Department of Energy Office of Nuclear Energy (DOE-NE) Advanced Fuels Campaign (AFC). Neutron irradiation in the High Flux Isotope Reactor (HFIR) is made possible by the Office of Basic Energy Sciences, US DOE. The report was authored by UT-Battelle under Contract No. DE-AC05-00OR22725 with the US DOE. Alicia Raftery and David Bryant performed most of the capsule assembly work. Doug Kyle and Alan Frederick performed the welding of the capsules and Eric Vidal performed the non-destructive examination of the capsules.

1. INTRODUCTION

Any new nuclear fuel concept must undergo rigorous irradiation testing so that a comprehensive knowledge base of fuel performance can be built to ultimately make the regulatory case to license the fuel. This has traditionally been accomplished by performing exhaustive integral fuel testing, including full- or near-full-scale testing under environmental conditions closely matching those of the intended application [1]. However, this logical approach presents some challenges that must be addressed. First, detailed analyses are required to properly design and characterize a full integral fuel test. This requirement requires significant time and cost when qualifying new fuels. Second, because integral tests are performed under prototypic conditions, the fission rate must also be matched to that of the intended application. This means that the time required to reach end-of-life burnup will take at least as long as the fuel would operate in its final application, and likely longer, because most test reactors operate at a much lower capacity factor than commercial reactors. Third, it is difficult to isolate a single fuel performance variable and develop a thorough scientific understanding of fuel performance during integral testing with so many interdependent variables. This lack of scientific understanding makes it extremely difficult to extend the use of a fuel that was tested under a specific set of conditions to other applications with different environmental conditions.

To accelerate the timeframe to qualify new nuclear fuels, a new, two-part approach is being developed that relies on modern modeling and simulation tools to rapidly identify parameters with a high impact on fuel performance and a large uncertainty. This data will allow for proper prioritization of targeted irradiation experiments. The second part of the approach to accelerated fuel qualification is to leverage separate effects irradiation tests. These tests will be designed specifically to isolate the most impactful fuel performance variables and provide experimental data to fill these critical gaps in the fuel performance models. Accordingly, Oak Ridge National Laboratory (ORNL) has developed and deployed a new experimental capability in the High Flux Isotope Reactor (HFIR): the MiniFuel irradiation vehicle [2-4]. This irradiation testing capability allows for highly accelerated burnup accumulation with minimal coupling between the fission rate and the fuel temperature. This is accomplished by reducing the volume of the fuel and packaging the miniature fuel specimens inside individually sealed capsules. The properly designed capsule ensures that the total nuclear heat generated inside each capsule is dominated by gamma heating in the structural components as opposed to fission heating in the fuel. This allows for a flexible irradiation vehicle that can accommodate a wide range of fuel compositions, enrichments, and even geometries. The small size of the fuel also greatly reduces temperature gradients, which allows for near-isothermal conditions.

The MiniFuel experiment vehicle has been successfully used to test a variety of sol gel-derived uranium nitride kernels and tristructural isotropic (TRISO)-coated particle fuels [5]. This document describes the successful assembly of the first set of MiniFuel targets containing monolithic fuel specimens that more closely resemble traditional UO_2 pellets. Two irradiation targets—each containing U_3Si_2 and reference UO_2 fuel disks—will be tested to a low ($\sim 8\text{--}10$ MWd/kg U) and moderate ($\sim 28\text{--}40$ MWd/kg U) burnup at temperatures in the range of $450\text{--}550^\circ\text{C}$. This report describes the fuel configuration and test matrix, the expected fuel burnup and temperature profiles, pre-irradiation characterization, experiment assembly, and plans for post-irradiation examination.

2. EXPERIMENT DETAILS

2.1 Fuel configuration and test matrix

The primary differences between the first MiniFuel experiments and the experiments described in this report are the fuel geometry and composition. The planned experiments discussed herein will test monolithic U_3Si_2 disks fabricated by Los Alamos National Laboratory (LANL), along with UO_2 disks fabricated at ORNL that will serve as a reference. The experiment geometry showing disk specimens contained inside sealed capsules is shown in Figure 1. The experiments described in this work will be inserted into two different baskets located in different inner small vertical experiment facilities in the permanent reflector of HFIR. Each target will be positioned in radial target position 2, facing away from the core centerline, and axial target position 1, at the vertical midplane of the core. Images of the U_3Si_2 and UO_2 disk specimens are shown in Figure 2 and Figure 3, respectively. The test matrix is summarized in Table 1.

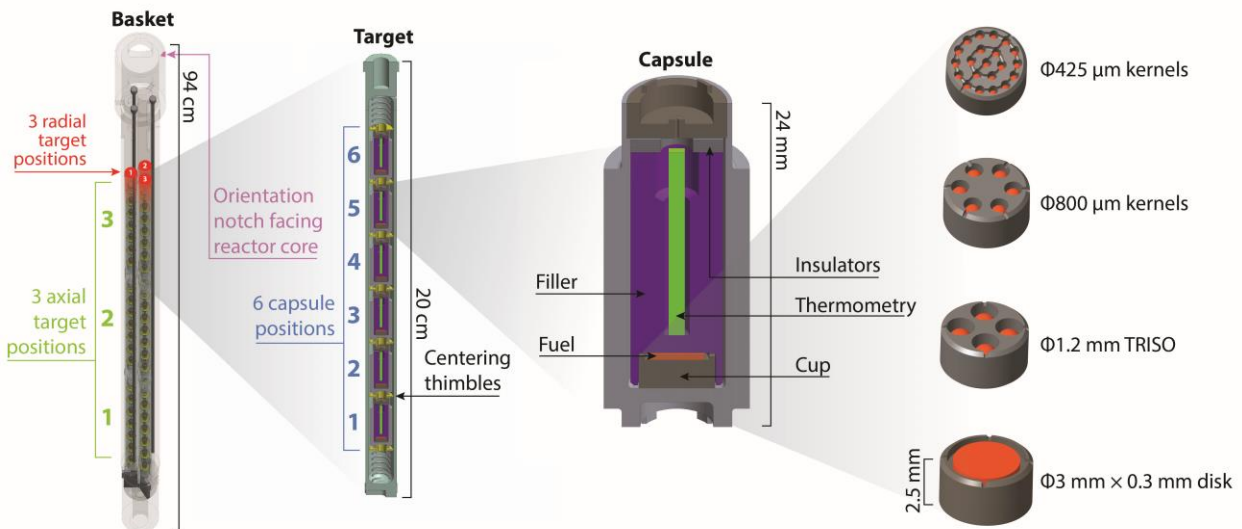


Figure 1. MiniFuel experiment configuration showing sealed capsules with disk specimens (this work), as well as other potential fuel configurations. This figure was reused with permission from Petrie et al. [2].

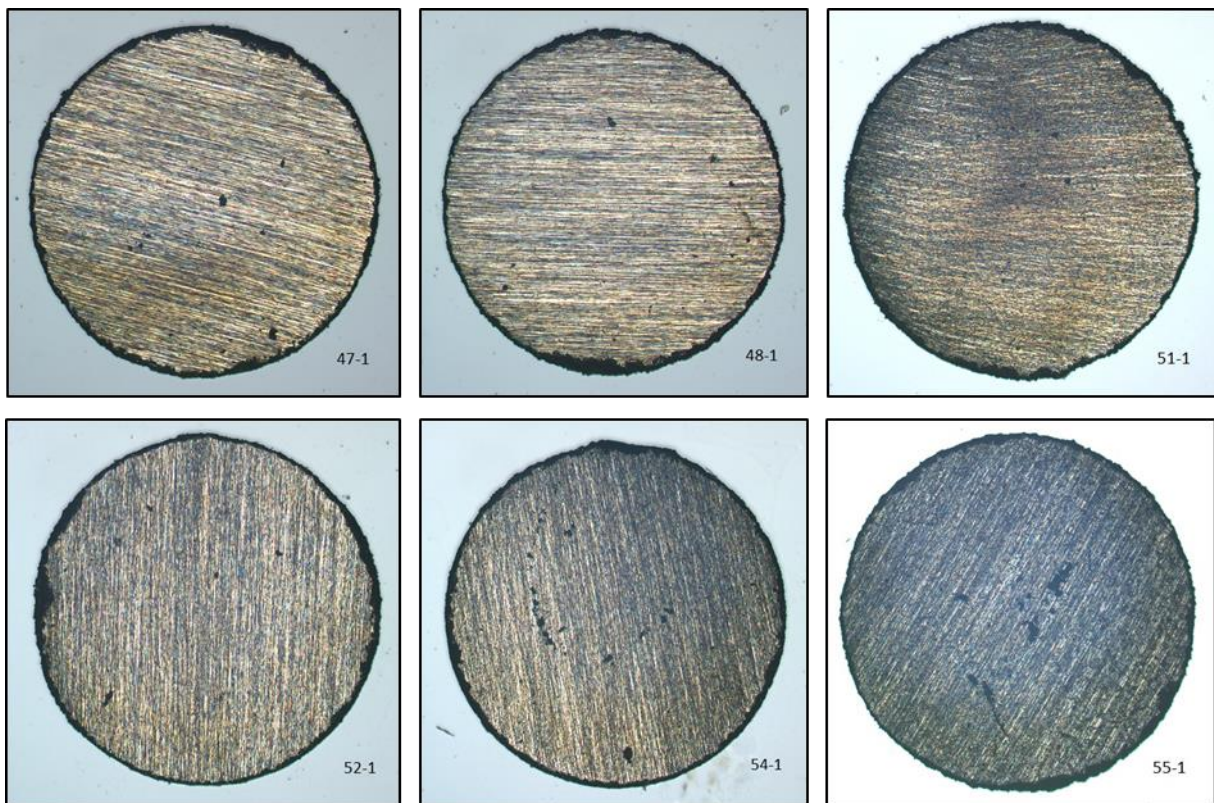


Figure 2. Pictures of the U_3Si_2 disk specimens [6].

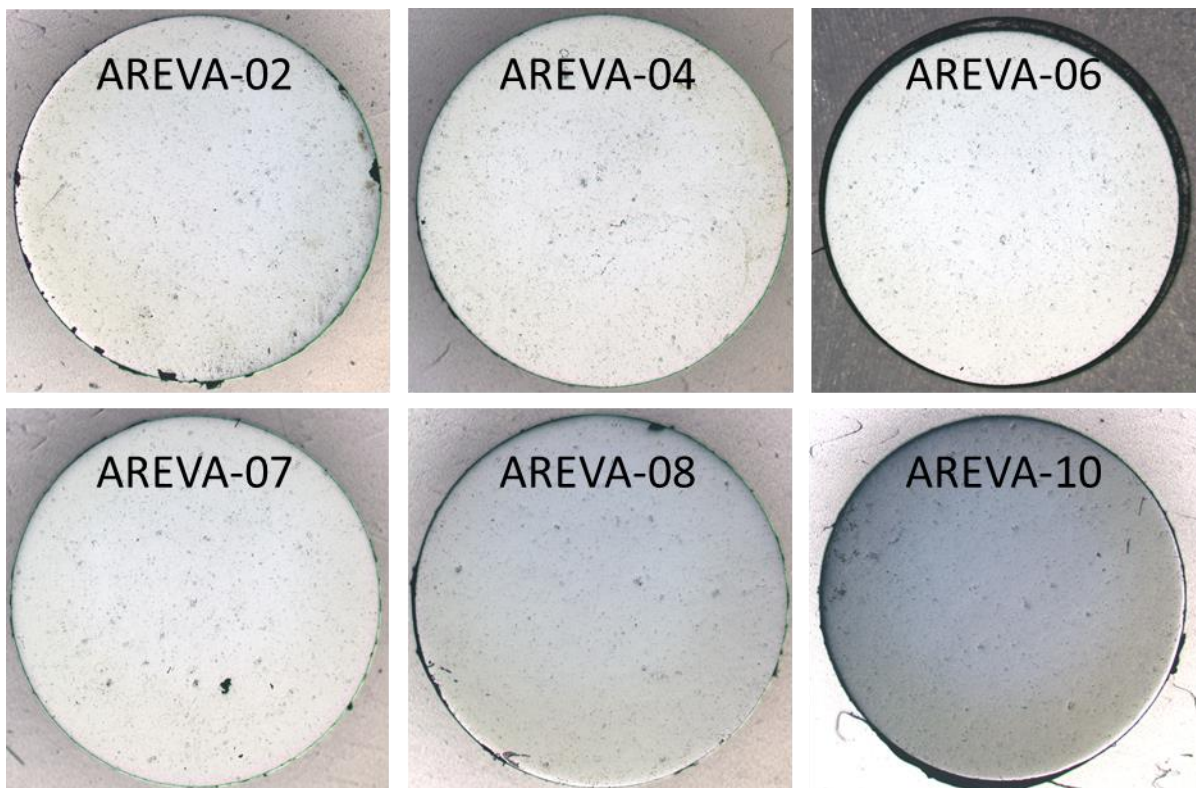


Figure 3. Pictures of the UO_2 disk specimens.

Table 1. Test matrix for U_3Si_2 and UO_2 monolithic disk irradiation.

Target ID	Fuel form	Fuel sample ID	²³⁵ U enrichment	Target burnup	Target temperature
LA01	UO ₂	AREVA-02	0.35 wt%	8–10 MWd/kg U	450–550°C
		AREVA-04			
		AREVA-06			
	U ₃ Si ₂	35-P-19-47	0.19 wt%		
		35-P-19-48			
		35-P-19-51			
LB02	UO ₂	AREVA-07	0.35 wt%	28–40 MWd/kg U	
		AREVA-08			
		AREVA-10			
	U ₃ Si ₂	35-P-19-52	0.19 wt%		
		35-P-19-54			
		35-P-19-55			

2.2 Pre-irradiation characterization

Pre-irradiation characterization included measurements of diameter, thickness, mass, and density (see Table 2). Additional unirradiated samples were preserved so that the irradiated and pre-irradiated microstructures can be compared. Dimensions for the U_3Si_2 specimens were measured independently by ORNL and LANL. At ORNL, diameter measurements were performed using calipers with 0.01 mm precision. Thickness measurements were performed using a micrometer with 0.001 mm precision. All samples were weighed using a scale. To determine density, volumes were calculated at ORNL using three different methods: (1) a simple geometric calculation using the measured diameter and thickness, (2) x-ray computed tomography (XCT) [7, 8], and (3) a wide area 3D optical profilometer (Keyence VR-5000). Geometric measurements performed at ORNL and LANL are labeled “ORNL Geo” and “LANL Geo,” respectively. Measurements made with the Keyence optical profilometer are labeled “Keyence.”

Dimensions of the UO_2 specimens were measured after pressing and sintering but before grinding. These pre-grinding measurements were used to determine the specimens’ geometric densities, because the larger specimen thickness could be measured more accurately. The reduced geometric accuracy post-grinding is evident when comparing the uncertainties in the geometric densities determined by ORNL for the U_3Si_2 specimens, which were measured after grinding, to the geometric densities for the UO_2 specimens, which were measured before grinding. It is possible that the outer regions of the specimens were more porous and that grinding these regions resulted in increased densities compared to the densities determined before grinding. All uncertainties are $\pm 2\sigma$ (95% confidence interval). The geometric uncertainties were determined via error propagation of the uncertainties in the measured diameters and thicknesses. Uncertainties are not reported for the Keyence measurements. LANL densities were determined geometrically after the specimens were ground to their final geometries using immersion density pre-grinding, although no uncertainties were reported for any of the measurements [6].

Figure 4 and Figure 5 show the percent theoretical densities determined for each UO_2 and U_3Si_2 specimen, respectively, using different techniques. The theoretical densities were assumed to be 10.96

and 12.20 g/cm³, respectively [9]. With a few exceptions, geometric measurements, XCT, and Keyence measurements generally give consistent volumes for the UO₂ specimens. Some XCT measurements predict densities >100% theoretical density, although the uncertainties are on the order of 5%. For the U₃Si₂ specimens, the Keyence measurements for specimens 52 and 54 are clearly nonphysical, with values close to 150% of theoretical density. It appears that the profilometer did not capture the thickness of these discs properly. The remaining densities are generally consistent across the various measurement techniques, although it is difficult to assess some of the data for which uncertainties are not reported. Geometric uncertainties are significantly greater for the U₃Si₂ specimens than the UO₂ specimens. This is due to larger variations in U₃Si₂ specimen thickness compared to the thickness variations in the UO₂ specimens. Efforts to resolve inconsistencies between the various techniques and to select the most appropriate techniques for pre- and post-irradiation density measurements are ongoing.

Table 2. Pre-irradiation mass and dimensional measurements of specimens.

Fuel sample ID	Fuel form	Mass (g)	Diameter (mm)	Thickness (mm)	Density (percent theoretical)				
					ORNL Geo	LANL Geo	LANL Immersion	XCT	Keyence
AREVA-02	UO ₂	0.0251	3.28	0.271	96.1±1.2	N/A	N/A	96.4±5.6	94.6
AREVA-04		0.0262	3.23	0.273	93.3±1.2	N/A	N/A	102.3±4.3	94.7
AREVA-06		0.0306	3.28	0.324	93.8±1.2	N/A	N/A	99.5±5.9	95.5
AREVA-07		0.0326	3.28	0.350	92.1±1.1	N/A	N/A	95.4±4.1	96.1
AREVA-08		0.0300	3.28	0.333	94.3±1.2	N/A	N/A	97.2±4.4	94.1
AREVA-10		0.0305	3.29	0.342	93.5±1.1	N/A	N/A	97.6±4.4	95.0
35-P-19-47	U ₃ Si ₂	0.0200	2.807	0.276	96.1±2.0	93.5	87.6	93.6±3.6	89.9
35-P-19-48		0.0186	2.807	0.255	96.8±7.7	94.3	89.5	89.3±3.3	90.3
35-P-19-51		0.0173	2.810	0.235	97.2±5.0	92.9	93.2	89.9±1.8	91.4
35-P-19-52		0.0180	2.827	0.245	96.0±2.2	95.5	91.1	101.3±2.4	149.9
35-P-19-54		0.0204	2.847	0.277	95.0±2.6	93.2	90.5	95.3±5.4	147.2
35-P-19-55		0.0189	2.813	0.268	93.0±5.2	92.9	90.6	89.1±4.1	91.0

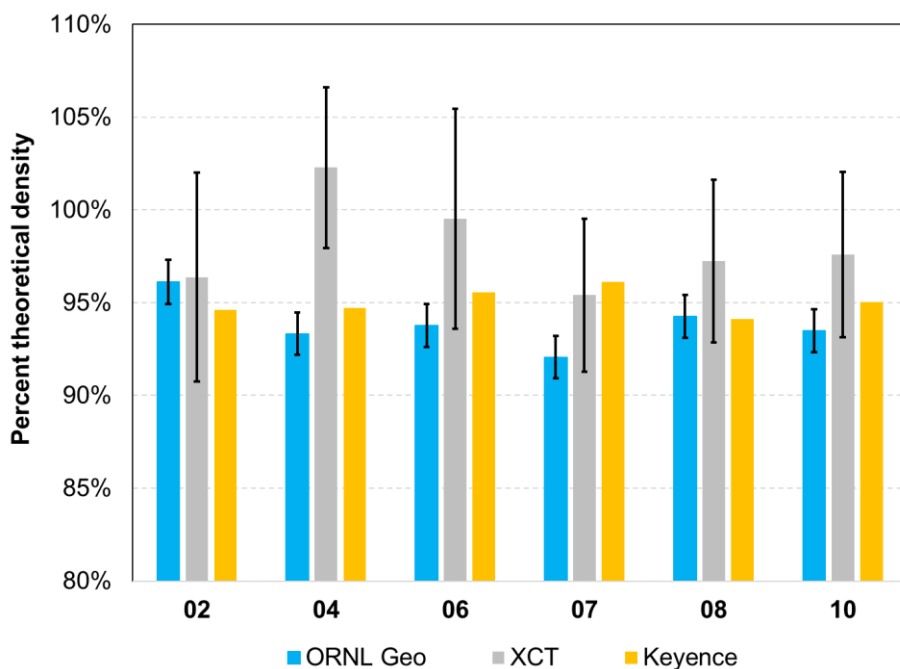


Figure 4. Percent theoretical densities for the UO₂ specimens determined using geometric measurements (ORNL Geo), XCT, and a 3D Keyence optical profilometer (Keyence). Only the last two digits of the specimen IDs are shown.

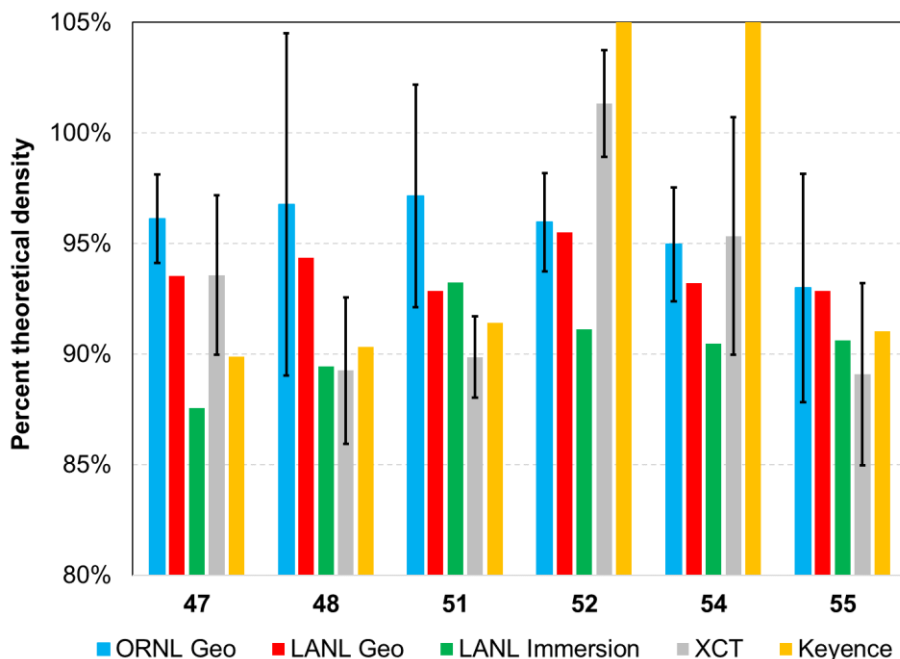


Figure 5. Percent theoretical densities for the U₃Si₂ specimens determined using geometric measurements (ORNL Geo and LANL Geo), immersion (LANL Immersion), XCT, and a 3D Keyence optical profilometer (Keyence). Only the last two digits of the specimen IDs are shown. Keyence measurements for specimens 52 and 54 are off scale and clearly nonphysical (>100% theoretical density).

3. EXPERIMENT ANALYSIS RESULTS

3.1 Burnup calculations

Fuel fission rates and burnup were calculated by coupling the MCNP and ORIGEN codes. Over time, the initial ^{235}U is burned, but breeding of fissile Pu isotopes allows for continued burnup accumulation with a fission rate that approaches an equilibrium after approximately 6 cycles of irradiation. Previous MiniFuel irradiations were inserted into the two radial target positions that face the center of the HFIR core. The monolithic fuel irradiations described in this report will be placed in the third radial position that faces away from the HFIR core. All targets will be placed at the axial midplane of the core. Moving radially away from the center of the core results in a slight reduction in the fission rates. Figure 6 shows fuel fission heating rates and accumulated burnup vs. the number of HFIR cycles for U_3Si_2 specimens fabricated from depleted uranium (0.22% ^{235}U). At this writing, burnup simulations have been performed for 4 cycles of irradiation. Simulations for up to 12 subsequent cycles are ongoing. The burnup, which is expressed per unit mass of uranium, is identical for UO_2 and U_3Si_2 specimens. Results are shown for various capsule positions within the irradiation target. The capsule positions are designated as follows:

- radial target position = R,
- axial target position = A, and
- subcapsule or capsule position = S.

RAS positions 121, 123, 124, and 126 are shown in Figure 6, covering the entire range of the irradiation target, from bottom to top. Based on these results, it is anticipated that after 4 cycles, a burnup of approximately 8 MWd/kg U will be reached. Because the fission rates typically approach an equilibrium after ~6 cycles [2], it is expected that after 12 cycles of irradiation, the total burnup will be approximately 28 MWd/kg U. The final burnup for target discharge will be determined by as-run HFIR operations and programmatic goals for accumulating burnup that is comparable to other experiments.

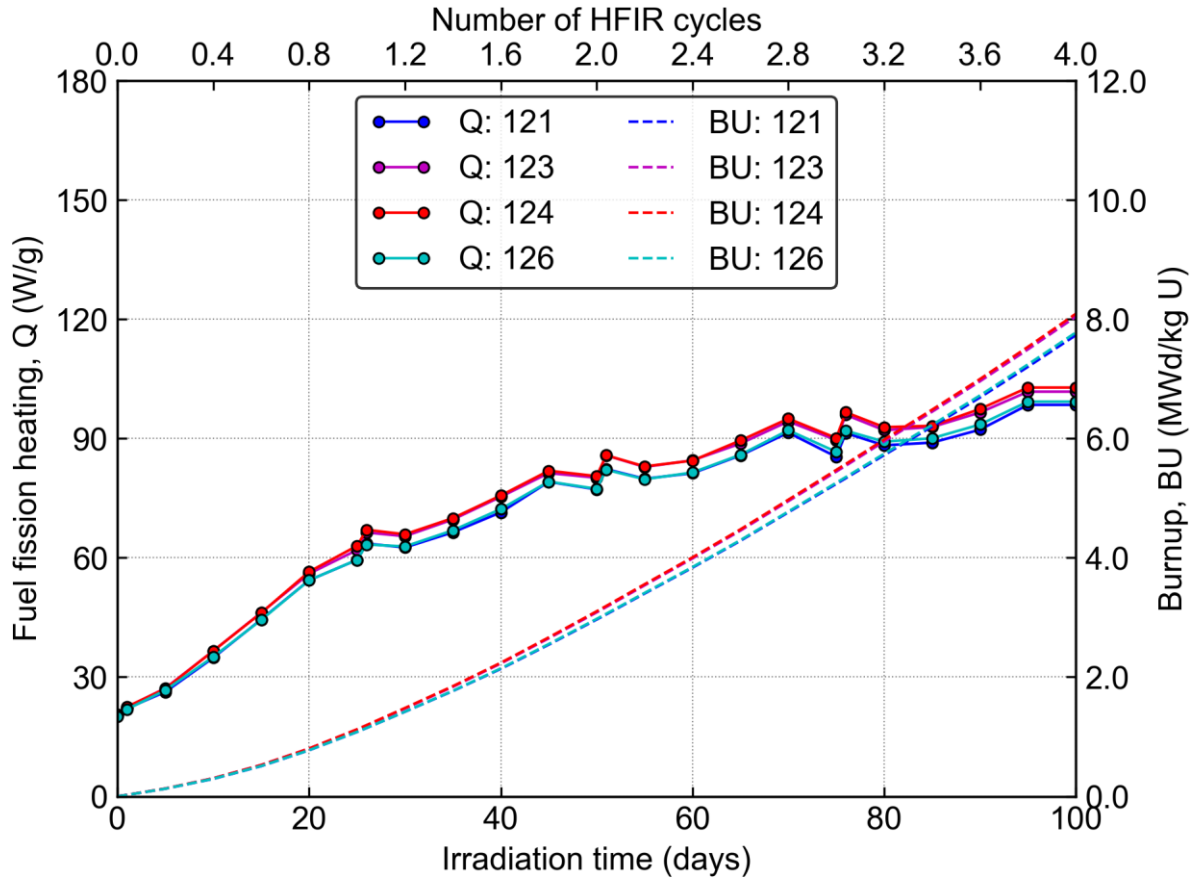


Figure 6. Calculated U_3Si_2 fuel fission rate (solid lines) and burnup (dashed lines) vs. irradiation time or number of HFIR cycles for the first 4 cycles of irradiation in capsules with RAS IDs 121, 123, 124, and 126. R = radial target position, A = axial target position, and S = subcapsule (or capsule) position.

3.2 Thermal analyses

Figure 7 shows temperature contours for a capsule containing U_3Si_2 fuel disks. These temperatures were calculated at the end of 4 cycles of irradiation in position RAS 123. Temperature is controlled by choosing the size of the gas gap between the capsules and the target housing, as well as the composition of the fill gas, which was chosen to be a 40.5% He–Ar balance mixture. The interiors of the capsules are filled with helium. The diameters of the capsules are nominally 9.20 mm, resulting in a nominal gas gap of 0.86 mm (10.06 mm inner target diameter). The average fuel temperature is approximately 542°C. The temperature gradients in the fuel are minimal (4°C) because of the small fuel size. The passive SiC temperature monitors (TMs) have an average temperature of approximately 514°C (~30°C lower than the fuel temperature) with temperature gradients of only ~2°C. The passive SiC TMs will be used to confirm the irradiation temperatures [10].

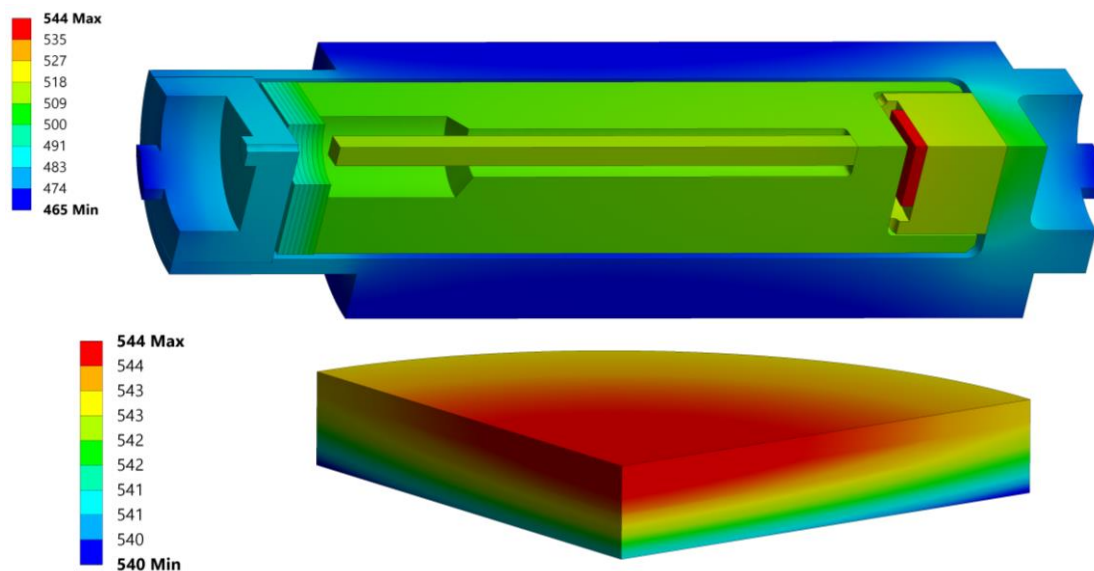


Figure 7. Predicted temperature contours (in °C) for a U_3Si_2 disk specimen in position RAS 123 at the end of 4 cycles of irradiation. Results show the capsule assembly (top) and the fuel specimen (bottom).

Figure 8 shows the average fuel and TM temperatures for all U_3Si_2 fuel specimens at beginning of cycle (BOC) and end of cycle (EOC) for cycles 1, 4, and 12. Temperatures for UO_2 specimens are very similar, as the fuel specimens have similar geometries and enrichments, and the MiniFuel experiment vehicle was specifically designed to be insensitive to variations in fuel heat load. The fuel temperature generally remains within the desired range of 450–550°C for most of the experiment. Fuel temperatures increase from BOC to EOC due to the withdrawal of the HFIR control plates. This increases the neutron and gamma flux in the reflector positions. For the MiniFuel experiments, the primary effect is an increase in gamma heating rates in the structural materials. There is also a small increase in fuel temperatures from Cycles 1–12 due to increases in fission heating resulting from breeding of plutonium isotopes (see Figure 6).

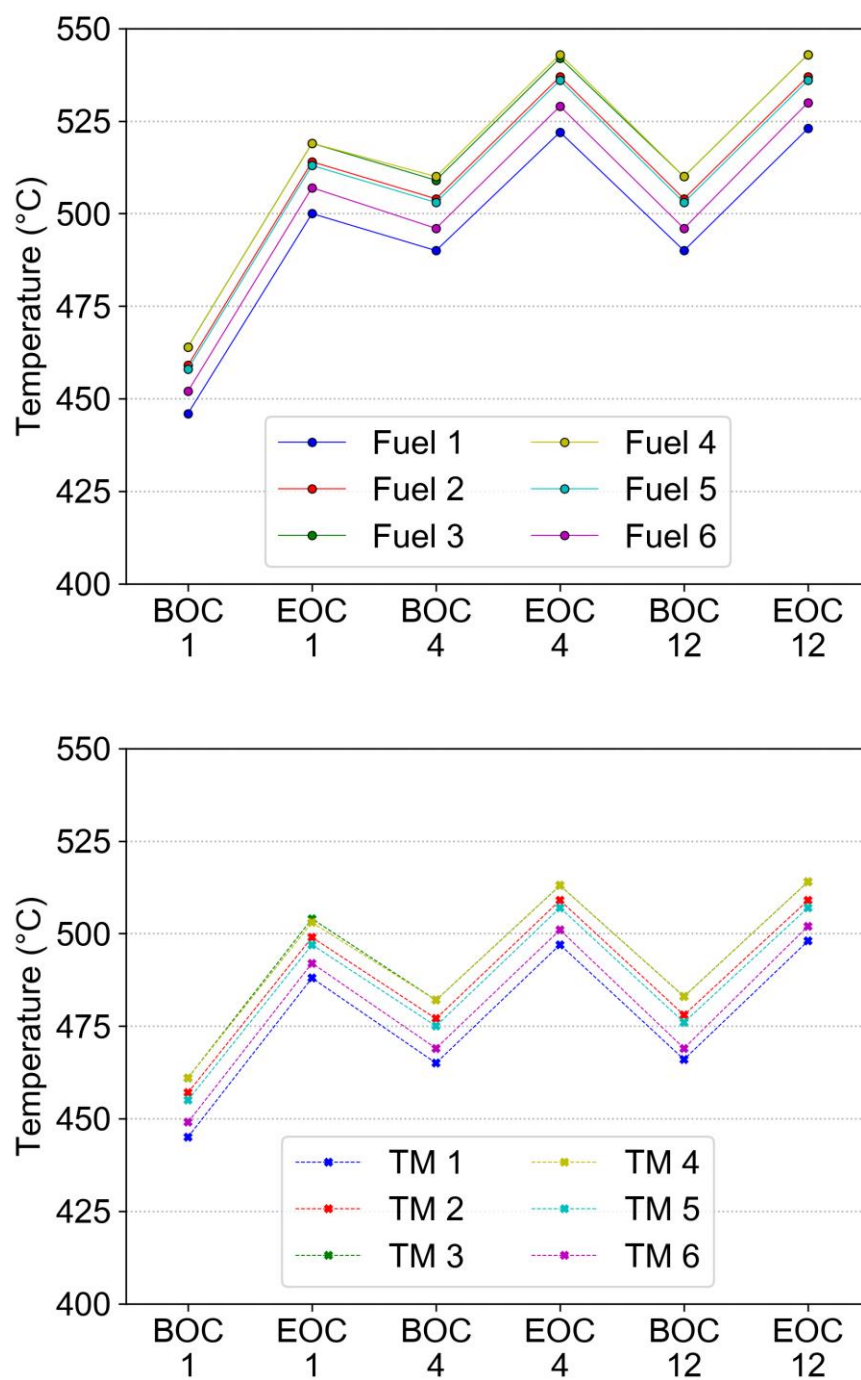


Figure 8. Calculated variations in the average U_3Si_2 disk fuel temperatures (top) and TM temperatures (bottom) at beginning of cycle (BOC) and end of cycle (EOC) for cycles 1, 4, and 12.

4. EXPERIMENT FABRICATION

As shown in Table 1 above, 12 fueled capsules were assembled. The parts layout for one capsule is shown in Figure 9. The components include a single fuel disk specimen (UO_2 shown), the capsule itself, and the capsule's endcap, cup, TM, filler, and insulators. The signed subassembly fabrication request forms are provided in Appendix A. All capsule components were dimensionally inspected and cleaned according to HFIR-approved procedures, drawings, and sketches.

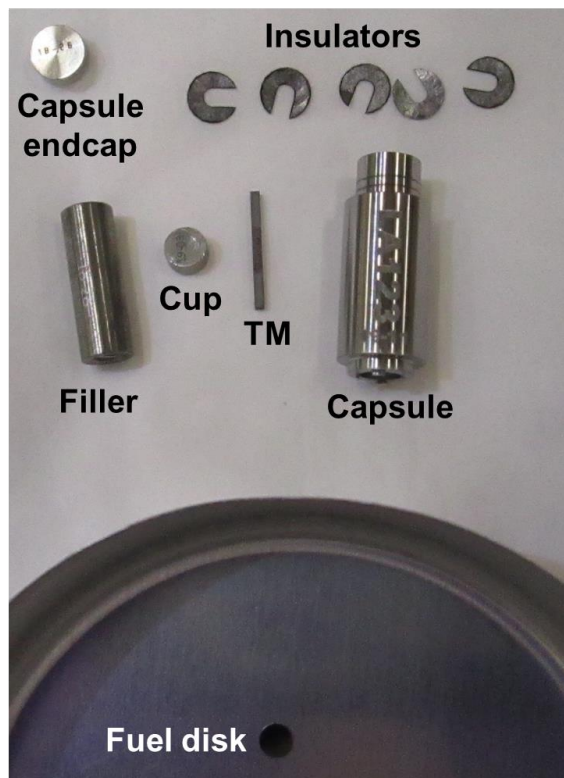


Figure 9. Components for one UO_2 -fueled capsule.

The fuel disks are loaded into the cup inside a custom bottom loading fixture as shown in Figure 10. After placing the fuel specimens in the cup, the filler is placed on top of the cup assembly, and the top loading fixture is used to apply pressure to the filler while it is flipped upside down, as shown in Figure 11 (a,b). The capsule is then flipped upside down and placed over the filler, as shown in Figure 11(c). The capsule is turned upright, and pressure is applied again with the top loading fixture to keep the internal components from moving. Figure 12 shows an upright capsule after inserting the TM (a), the insulators (b), and the endcap (c). Lines were engraved into the upper regions of the capsules to identify the location where each capsule should be punctured after irradiation, to measure fission gas release, and then cut open.

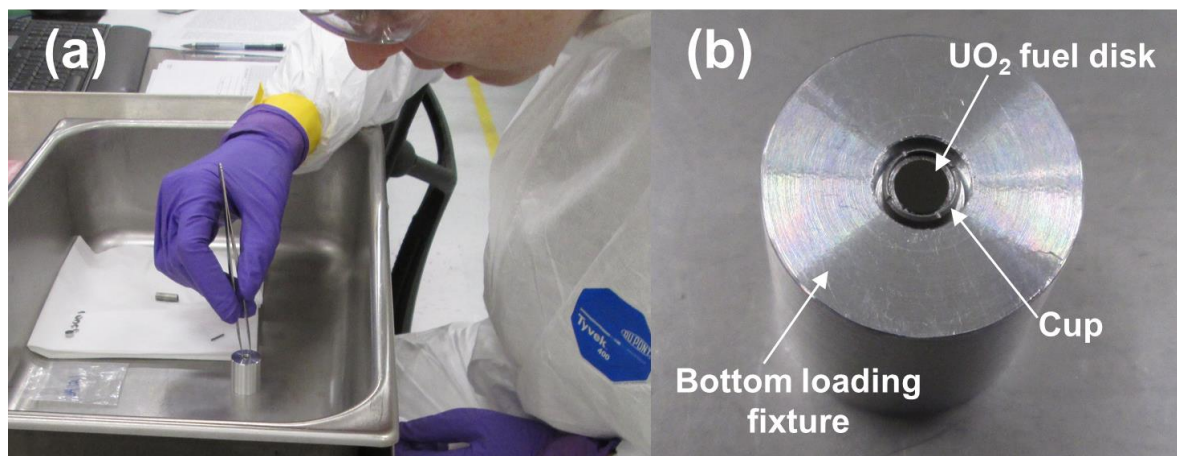


Figure 10. Loading of a UO₂ disk specimen (a) into a cup inside the bottom loading fixture (b).

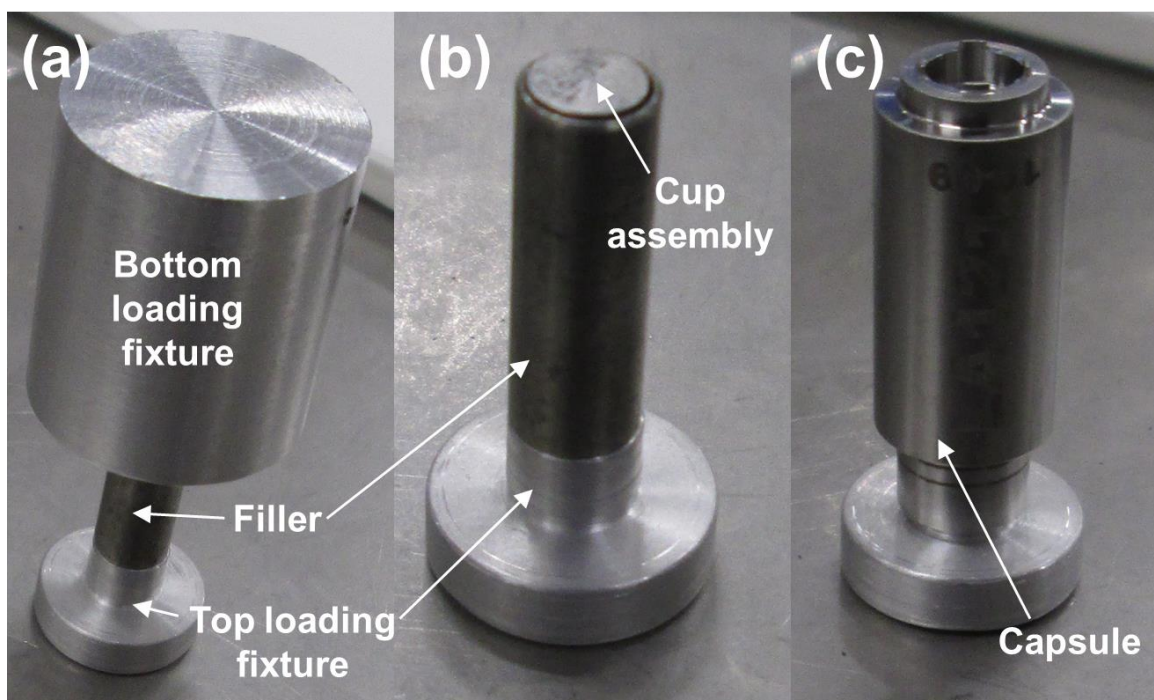


Figure 11. Filler placed over cup assembly and turned upside down while applying pressure with top loading fixture (a), bottom loading fixture removed (b), and capsule is turned upside down and placed over the tube and cup assembly (c).

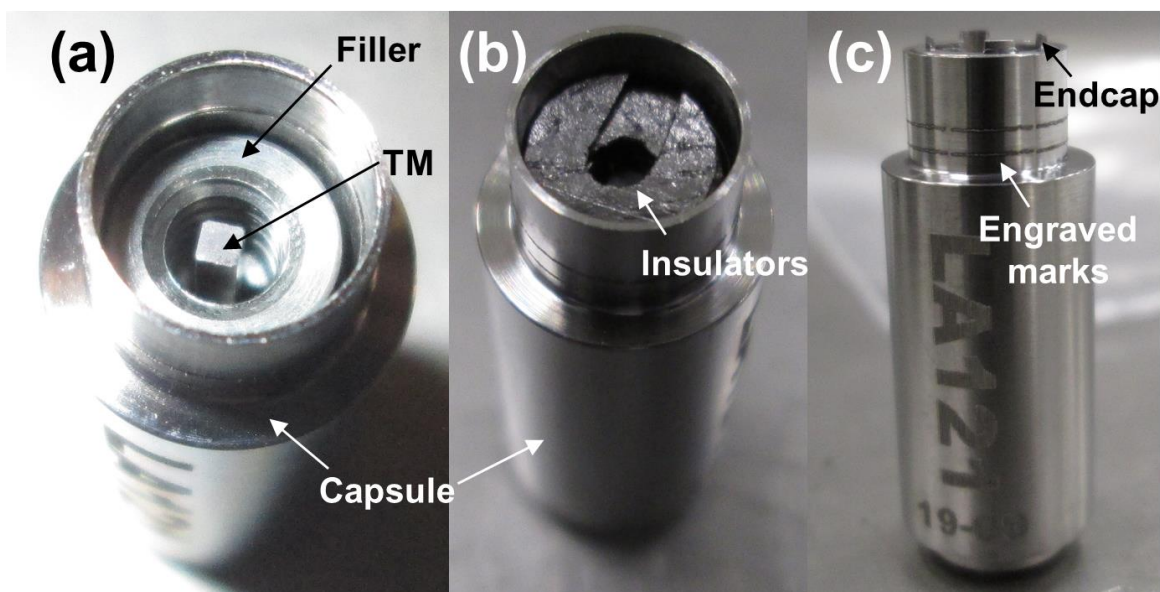


Figure 12. Loading TMs (a), insulators (b), and endcaps (c) into a capsule.

After the internal components were assembled, all capsule endcaps were welded to the capsule bodies using an electron beam weld (see Figure 13). The capsule assemblies were then placed inside sealed containers that were evacuated and backfilled with ultra-high-purity helium three times to ensure a pure environment. The containers were placed inside a glove box, which was also evacuated and backfilled with the same gas used in the sealed containers. Each capsule's end cap has a small hole that was seal-welded using a gas tungsten arc welding procedure. All welds passed visual examination. Each capsule was then sent for nondestructive examination, which included a bubble test and a helium leak test. All assemblies passed the nondestructive examination (see Appendix A).

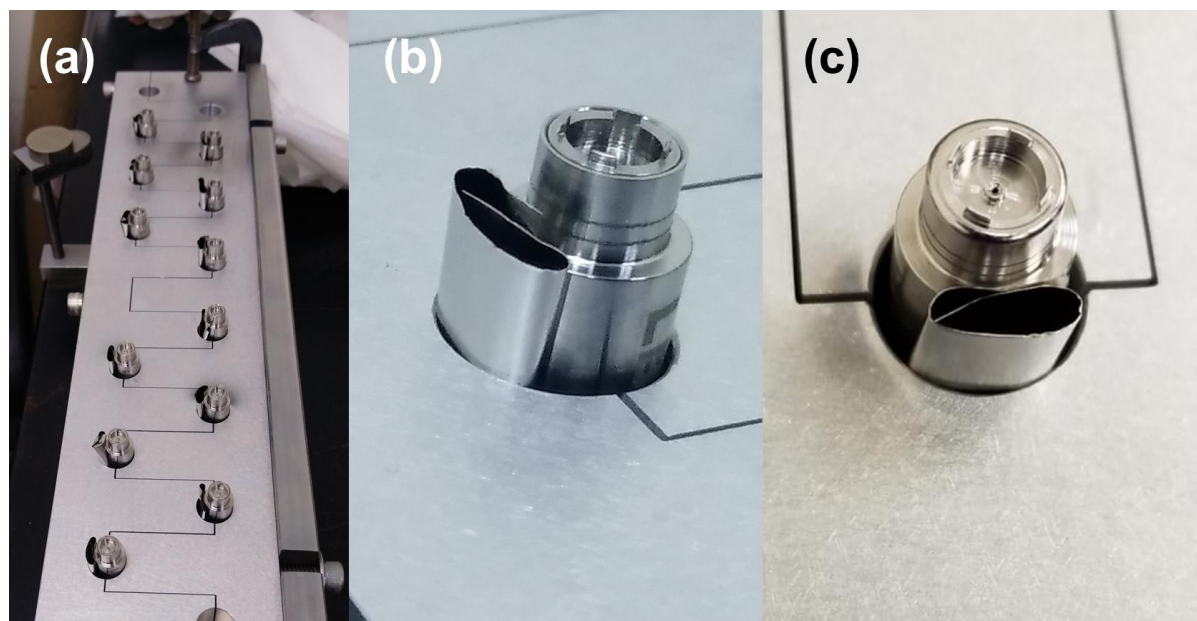


Figure 13. All 12 capsules prepped for electron beam welding (a); close-up views of a single capsule before (b) and after (c) welding.

5. PLANNED POST-IRRADIATION EXAMINATION

The first target (LA01) will be irradiated to a nominal burnup of 8–10 MWd/kg U, which corresponds to 4–5 cycles of irradiation. After a few months of cooling, the LA01 target will be shipped to the Irradiated Fuels Examination Laboratory (IFEL) for disassembly in the late calendar year 2020 timeframe. The higher burnup target (LB02) is scheduled for 12 or more cycles of irradiation, which corresponds to a nominal burnup of 28 MWd/kg U or higher. The final discharge burnup for LB02 will depend on results from LA01 and results from other U_3Si_2 irradiations. The tentative date for shipping LB02 is some time during calendar year 2022. After the targets are received at IFEL, they will be cut open with a slow-speed saw to extract the individual capsules. The capsules will then be punctured in a specially designed apparatus to collect the released ^{85}Kr fission gases. The ^{85}Kr gases will be frozen in cold traps, and then gamma counting of the traps will be performed to measure the ^{85}Kr content, and thus the fission gas release [8]. The capsule endcaps will be cut using a slow-speed saw so that the TMs and fuel specimens can be extracted. The fuel will be transferred to separate facilities to measure mass and volume. Measurements will likely be taken using XCT [7], which will allow for determination of fuel swelling. Finally, the specimens will be prepared for microstructural characterization using optical and electron microscopy.

6. SUMMARY AND CONCLUSIONS

This report summarizes the first successful fabrication of MiniFuel capsules loaded with monolithic ATF samples under AFC. U_3Si_2 and UO_2 samples were successfully assembled into capsules, welded, nondestructively tested, and are now ready for insertion into the HFIR during cycle 487 (April 2020). These monolithic fuel disks will be evaluated post-irradiation to determine swelling, fission gas release, and microstructural evolution. This report describes the test matrix and the pre-irradiation specimen characterization, including pictures of the specimens and the capsule assembly process. One of the key challenges moving forward will be to choose the appropriate technique to accurately quantify the physical density of these small fuel samples so that fuel swelling can be accurately determined. The data that will be collected from this experiment will complement current integral tests of U_3Si_2 being performed in the Advanced Test Reactor and will ultimately inform fuel performance modeling of U_3Si_2 for light-water reactor applications. The inclusion of monolithic UO_2 specimens in a MiniFuel experiment will provide the first opportunity to benchmark MiniFuel experiments against the large amount of UO_2 fuel performance data that has been collected over many decades.

7. REFERENCES

1. Crawford, D. C. et al., "An approach to fuel development and qualification," *Journal of Nuclear Materials*, **371** (2007) pp. 232-242.
2. Petrie, C. M., J. R. Burns, A. M. Raftery, A. T. Nelson and K. A. Terrani, "Separate effects irradiation testing of miniature fuel specimens," *Journal of Nuclear Materials*, **526** (2019) pp. 151783.
3. Petrie, C. M., J. Burns, R. N. Morris and K. A. Terrani, "Miniature Fuel Irradiations in the High Flux Isotope Reactor," In *40th Enlarged Halden Programme Group Meeting*. 2017: Lillehammer, Norway.
4. Petrie, C. M., J. Burns, R. N. Morris and K. A. Terrani, "Small-Scale Fuel Irradiation Testing in the High Flux Isotope Reactor," In *Water Reactor Fuel Performance Meeting 2017*. 2017: Jeju Island, Korea.
5. Petrie, C. M. et al., *Irradiation of Miniature Fuel Specimens in the High Flux Isotope Reactor*, ORNL/SR-2018/844, Oak Ridge National Laboratory: Oak Ridge, TN (2018).
6. Abdul-Jabbar, N. M. and J. T. White, *Processing and Characterization of U_3Si_2 at the MiniFuel Scale*, LA-UR-19-23733, Los Alamos National Laboratory: Los Alamos, NM (2019).
7. Richardson, M. D., G. W. Helmreich, A. M. Raftery and A. T. Nelson, *Resolution capabilities for measurement of fuel swelling using tomography*, ORNL/SPR-2019/1071, Oak Ridge National Laboratory: Oak Ridge, TN (2019).
8. Raftery, A. M. et al., *Development of a characterization methodology for post-irradiation examination of miniature fuel specimens*, ORNL/SPR-2018/918, Oak Ridge National Laboratory: Oak Ridge, TN (2018).
9. Remschnig, K., T. Le Bihan, H. Noël and P. Rogl, "Structural chemistry and magnetic behavior of binary uranium silicides," *Journal of Solid State Chemistry*, **97** (1992) pp. 391-399.
10. Field, K. G., J. L. McDuffee, J. W. Geringer, C. M. Petrie and Y. Katoh, "Evaluation of the continuous dilatometer method of silicon carbide thermometry for passive irradiation temperature determination," *Nuclear Instruments and Methods in Physics Research Section B: Beam Interactions with Materials and Atoms*, **445** (2019) pp. 46-56.

APPENDIX A. FABRICATION DOCUMENTATION FOR EXPERIMENTS

Monolithic ATF MiniFuel Sample Capsules Ready for HFIR Insertion

A-2

January 17, 2020

Capsule Fabrication Request Sheet

Page 1 of 1
Date 1/9/2020

Target ID: LA01

Irradiation Conditions

Irradiation Location (R, A) 1 2

Number cycles 4

First Cycle Goal 487

Fill Gas He

Irradiation Temperature 500°C

Holder assembly drawing S17-13-CER_FUEL, Rev. 2

Approvals

Request	Build
Performed by: <u>NASA</u> 1/10/20	<u>Shirley Kaffery</u> 1/10/20
Checked by: <u>Petrie, Christian M. (rcp)</u>	<u>David B. Smith</u> 1/10/20

Digitally signed by Petrie, Christian M. (rcp)
Location:
Date: 2020-01-10 14:52:16

Holder Assembly							Component IDs for each holder ID						Component mass (g) for each holder ID							
Component	Drawing	Rev.	Part	Material	MAT IR	FAB IR	LA121	LA122	LA123	LA124	LA125	LA126	LA121	LA122	LA123	LA124	LA125	LA126	All	
Holder	S17-14-CER_FUEL	2	1	Ti-6Al4V	21033	21047	19-09	19-10	19-11	19-12	19-13	19-14	3.3088	3.2764	3.2703	3.2702	3.2747	3.2707	19.6711	
End cap	S17-14-CER_FUEL	2	2	Ti-6Al4V	20803	20805	18-24	18-25	18-26	18-27	18-28	18-29	0.2234	0.2226	0.2255	0.2244	0.2228	0.2232	1.3419	
Tube	S17-13-CER_FUEL	2	2	Moly	20611	20806	18-26	18-27	18-28	18-29	18-30	18-32	3.3327	3.3354	3.3389	3.3598	3.3502	3.3381	20.0551	
Thermometry	S17-13-CER_FUEL	2	3	SiC	20863	21048	19-01	19-02	19-03	19-04	19-05	19-06	0.0434	0.0437	0.0435	0.0434	0.0431	0.0435	0.2606	
Insulator disks (list total # and mass)	S17-13-CER_FUEL	2	4	Grafoil	19812	19812	5 pcs	5 pcs	5 pcs	5 pcs	5 pcs	5 pcs	0.0125	0.0127	0.0128	0.0127	0.0118	0.0125	0.0750	
Disk fuel dish	S17-26-CER_FUEL	2	2	Moly	20611	21050	19-01	19-02	19-03	19-04	19-05	19-06	0.3815	0.3575	0.3833	0.3643	0.3629	0.3646	2.1741	
Disk fuel specimen	S17-26-CER_FUEL	2	3	UO2	20818	20818	Areva-02	Areva-04	Areva-06	N/A	N/A	N/A	0.0251	0.0262	0.0306	N/A	N/A	N/A	0.0819	
Disk fuel specimen	S17-26-CER_FUEL	2	3	U3Si2	20818	20818	N/A	N/A	N/A	35-P-19-47	35-P-19-48	35-P-19-51	N/A	N/A	N/A	0.0200	0.0186	0.0173	0.0559	
Total													7.3074	7.2745	7.2849	7.2948	7.2841	7.2699	43.7158	
Fuel													0.0251	0.0262	0.0306	0.0200	0.0186	0.0173	0.1378	

Capsule fabrication request sheet for target LA01.

Capsule Fabrication Request Sheet

Page 1 of 1
Date 1/9/2020

Target ID: LB02

Irradiation Conditions

Irradiation Location (R, A) 1 2

Number cycles 12

First Cycle Goal 487

Fill Gas He

Irradiation Temperature 500°C

Holder assembly drawing S17-13-CER_FUEL, Rev. 2

Approvals

Performed by:


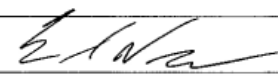
Checked by:

Request	Build
<i>[Signature]</i> 1/10/20	<i>[Signature]</i> 1/10/20
Petrie, Christian M. (rcp)	<i>[Signature]</i> 1/10/2020

Holder Assembly

Component	Drawing	Rev.	Part	Material	MAT IR	FAB IR	Component IDs for each holder ID						Component mass (g) for each holder ID						All
							LB121	LB122	LB123	LB124	LB125	LB126	LB121	LB122	LB123	LB124	LB125	LB126	
Holder	S17-14-CER_FUEL	2	1	Ti-6Al4V	21033	21047	19-15	19-16	19-17	19-18	19-19	19-20	3.2927	3.2738	3.2708	3.2706	3.2740	3.2539	19.6358
End cap	S17-14-CER_FUEL	2	2	Ti-6Al4V	20803	20805	18-18	18-19	18-20	18-21	18-22	18-23	0.2255	0.2216	0.2242	0.2233	0.2245	0.2238	1.3429
Tube	S17-13-CER_FUEL	2	2	Moly	20611	20806	18-33	18-34	18-35	18-36	18-37	18-38	3.3451	3.3320	3.3359	3.3660	3.3286	3.3584	20.0660
Thermometry	S17-13-CER_FUEL	2	3	SiC	20863	21048	19-07	19-08	19-09	19-10	19-11	19-12	0.0436	0.0436	0.0437	0.0435	0.0432	0.0434	0.2610
Insulator disks (list total # and mass)	S17-13-CER_FUEL	2	4	Grafoil	19812	19812	5 pcs	5 pcs	5 pcs	5 pcs	5 pcs	5 pcs	0.0125	0.0126	0.0125	0.0122	0.0124	0.0119	0.0741
Disk fuel dish	S17-26-CER_FUEL	2	2	Moly	20611	21050	19-07	19-08	19-09	19-10	19-11	19-12	0.3642	0.3608	0.3583	0.3631	0.3646	0.3605	2.1715
Disk fuel specimen	S17-26-CER_FUEL	2	3	UO2	20818	20818	Areva-07	Areva-08	Areva-10	N/A	N/A	N/A	0.0326	0.0300	0.0305	N/A	N/A	N/A	0.0931
Disk fuel specimen	S17-26-CER_FUEL	2	3	U3Si2	20818	20818	N/A	N/A	N/A	35-P-19-52	35-P-19-54	35-P-19-55	N/A	N/A	N/A	0.0180	0.0204	0.0189	0.0573
Total													7.3162	7.2744	7.2759	7.2967	7.2677	7.2708	43.7017
Fuel													0.0326	0.0300	0.0305	0.0180	0.0204	0.0189	0.1504

Capsule fabrication request sheet for target LB02.

		ORNL Surveillance & Inspection Organization - Certificate #4121.01/Scope of Accreditation to ISO/IEC 17020:2012		Report Number: 11/13/20-1	
LEAK TEST REPORT					
Test Requested by: D. BRYANT			Allowable Leak Rate: $< 1.0 \times 10^{-7}$ Std-Atm-cc/s		
Date Requested: 12/10/19			Date Required: 12/11/19		
Work Order Number: 3838487			Test Pressure Req. Across Boundary: -1 Atm		
Item Tested: 12 EA. MINIFUEL CAPSULES			Customer: -		
Specification: 517-13-CER-FUEL RZ		NDE 70, Rev: 7	Technique Used: INSIDE-OUT	Rev: 0	<input checked="" type="checkbox"/> Inside - Out <input type="checkbox"/> Outside - In
EQUIPMENT					
LEAK DETECTOR			STANDARD LEAK		
Make and Model: ADIXEN ASM 340			Manufacturer: VERLO		Tracer Gas: He
Serial Number: HLD 1601393			Model: SC-4		Serial Number: 18091
			Leak Rate: 2.57×10^{-8} Atm-cc/s @ -1 atm @ 23.5 °C		
TEST GAUGES			Correlation Formula: $[1 - (T_{cal} - T_{sur}) C_T] LR$		
Temp Gauges: A001957		Due: 7/30/20	Correlated LR: 2.5×10^{-8} Atm-cc/s @ -1 atm @ 22.6 °C		
Pressure Gauges: -		Due: -	Calibration Due Date: 10/1/20		
RESULTS <input checked="" type="checkbox"/> Quantitative <input type="checkbox"/> Semi - Quantitative					
MACHINE CALIBRATION			SYSTEM TEST CONDITIONS		
System Pressure: 2.3×10^{-2} mb			System Temperature: 22.6 °C <input checked="" type="checkbox"/> Surface <input type="checkbox"/> Internal Gas		
Background: $< 1.0 \times 10^{-9}$ Atm-cc/s			delta P Test Boundary: -1 Atm		
Leak Response: 2.5×10^{-8} Atm-cc/s			Tracer Gas: He		% Concentration: 100
Minimum Detectable Leak: 1.0×10^{-9} Atm-cc/s			System Response Time: ~5s		
System Sensitivity: 2.0×10^{-9} Atm-cc/s			System Response: 2.7×10^{-9} Atm-cc/s		
Response Time: ~5s			Duration of Test: ~30s		
Aux. Equipment:					
<input checked="" type="checkbox"/> ACCEPT <input type="checkbox"/> REJECT <input type="checkbox"/> SKETCH / DATA ATTACHED			System Leak Rate: $< 1.0 \times 10^{-7}$ Atm-cc/s @ -1 atm @ 22.6 °C		
COMMENTS:					
FINE LT LA121 → 126 LB121 → 126					
Test Conducted By: E. VORL 					
Level: III		Date: 01/13/2020		Time: 3:00	
Form NDE 70-MS, Rev. 1 CN02		IDMS: 21077			

Helium leak testing results for all capsules

Monolithic ATF MiniFuel Sample Capsules Ready for HFIR Insertion

January 17, 2020

A-5



ORNL Surveillance and Inspection Organization / Certificate #4121.01 /
Scope of Accreditation to ISO/IEC 17020:2012

Report Number: 1/13/20-3

LEAK TEST REPORT - BUBBLE TEST

Test Requested by: D. BRYANT	Customer: -
Date Requested: 12/10/19	Date Required: 12/11/19
Work Order Number: 3838487	NDE 70, Rev: 7 Tech, NDE 70 - BT Rev: 0
Item Tested: 12 EA. MINI FUEL CAPSULES	Test Pressure Required: -1 ATM
Specification: 517-13-CER-FUEL R.2	Inspection Criteria: NO BUBBLES @ 2 MIN
Technique Used: VAL BOX	Liquid Media Used: IMMERSIT C/M 200 @ 20% SW
Test Gas Used: VAL	Liquid Applicator Type: IMMERSION
Inspection Light Intensity: >100 FC	Post Cleaning Method: DI RINSE - DRY
Other Apparatus Used:	

Direct Pressure Technique ☐

Vacuum Pressure Technique ☒

Component Limits of Test:

Component Test Site 5500

Component Installation Site

Gauges				Test Pressure		Temperature	
Mfg	ID No	Calibration Date	Range	Beginning	End	Beginning	End
	A002126	8/26/19	0-30" Hg	15" Hg	15" Hg	-	-

Temperature Measuring Device

Mfg.	Model	Range	I.D. Number

RESULTS

☒ ACCEPT

☐ REJECT

POST CLEANING PERFORMED:

☒ Y ☐ N

Comments:

GROSS LT

LA121 → 126

LB121 → 126

Test Conducted By:

E. VIOAC *[Signature]*

Level: TIF

Insp. Date: 01/13/2020

Form NDE-70-Bubble Rev. 1 CN02

IDMS: 10960

Bubble testing results for all capsules